

# Silk-based antimicrobial peptide mixed with recombinant spidroin creates functionalized spider silk

Frank Y.C. Liu<sup>1</sup>

Keywords: Spider silk, silk sutures, surgical site infection, synthetic silk, antimicrobial peptide

## 1. Abstract

Surgical site infection (SSI) from sutures is a global health emergency because of the antibiotic crisis. Methicillin-resistant *S. aureus* and other emerging strains are difficult to treat with antibiotics, so drug-free sutures with antimicrobial properties are a solution. Functionalized spider silk protein (spidroin) is a candidate for its extraordinary strength because it has a large repetitive region (150Rep) that forms crosslinked beta-sheets. The antimicrobial peptide HNP-1 can be connected to recombinant spidroin to create antimicrobial silk. Ni-NTA purified 2Rep-HNP1 fusion protein was mixed with recombinant NT2RepCT spidroin at 1:25, 1:20, 1:10 ratios, and spun into silk fibers by syringe-pumping protein into a 100% isopropanol bath. Beta-sheet crosslinking of the identical 2Rep regions tagged the 2Rep-HNP1 permanently onto the resultant silk. Silk showed no sign of degradation in an autoclave, PBS, or EtOH. The tagged 2Rep-HNP1 retained broad-spectrum antimicrobial activity >90% against *S. aureus* and *E. coli* as measured by log reduction and radial diffusion assay. Furthermore, a modified expression protocol increased protein yield of NT2RepCT 2.8-fold, and variable testing of the spinning process demonstrated the industrial viability of silk production. We present a promising suture alternative in antimicrobial recombinant spider silk.

## 2. Introduction

Surgical site infections (SSI) are a serious health problem worldwide, representing more than 20% of the 4.1 million cases of healthcare-associated infections in the EU each year.[1] *Staphylococcus aureus*, specifically the methicillin-resistant strain (MRSA), is now the leading cause of SSI in the US.[2] This poses a significant economic burden to patient hospital care, averaging \$25k to patients in the US.[3, 4] SSI often come through contamination of sutures and

28 other equipment, because they can act as a reservoir for infection.[5] The traditional strategy to  
29 prevent SSI is to inject antibiotics to the surgery site, and newer methods improve on this by  
30 incorporating coatings on sutures, but all still rely on antibiotics.[5-7] The excessive use of  
31 antibiotics to treat microbial infections, however, has led to resistant strains that reduce the  
32 effectiveness of treatments, leading to the antibiotic crisis.[8] As such, there is a dire need to  
33 research alternatives to antibiotic-based sutures that are less likely to develop bacteria resistance  
34 in order to decrease SSI.[5, 9-11]

35 Antimicrobial peptides, polycationic polymers, silver ions, and have been shown to be effective  
36 coatings.[12-14] Antimicrobial peptides (AMP) display broad-spectrum antimicrobial activity  
37 regardless of antibiotic resistance, and have been shown to display antibiofilm properties as well,  
38 making them a good candidate.[15] Furthermore, their cell wall-based mode of action, and the  
39 countless AMP motifs they present make bacterial resistance less likely.[16] However, concern  
40 about toxicity in humans has hindered their development.[16] Human neutrophil defensin 1  
41 active peptide (HNP-1) derived from the innate immune system resolves this issue.[17] It is  
42 effective against a broad range of microorganisms such as *E. coli* with a preference towards  
43 Gram-positive bacteria including *S. aureus*, while also having low toxicity against mammalian  
44 cells, demonstrated in in vivo studies against *M. tuberculosis*. [18-21]

45 Aside from attachments or coatings, the suture can be improved as well with novel polymers,  
46 notably spider silk, the strongest known biomaterial.[22, 23] The synthesis of multifunctional  
47 silk using specific silk glands to assist in reproduction and predation is a unique ability of spiders  
48 following more than 380 million years of evolution.[24, 25] Spiders produce a silk with high  
49 tensile strength, temperature resilience, and bio-compatibility that makes it a superior material  
50 for medical sutures.[26-29] Spider silk proteins (spidroins) (Fig. 1A) consist of nonrepetitive N  
51 and C terminals shown to aid silk formation, and extensive repetitive regions in between that  
52 contribute to the properties of the silk.[30-36] For example, major ampullate spidroin has poly-A  
53 motifs in the repetitive region (Rep) that forms into crosslinked beta-sheets, giving the silk  
54 incredible strength.[37, 38]

55 With *E. coli* protein expression systems growing in popularity, it is now cost-effective to produce  
56 recombinant spidroins. Smaller recombinant spidroins (minispidroins) with a reduced repetitive  
57 region can have much higher protein yields without compromising strength.[39] The chimeric  
58 minispidroin NT2RepCT (Fig. 1B) is a well-studied example that adds chimeric terminals with  
59 extreme solubility to increase yield further, up to 125mg/L.[35] To biomimetically spin  
60 NT2RepCT, a syringe pump pushes NT2RepCT into a coagulating bath (pH=5, isopropanol, or  
61 methanol) with sufficient shear force, which is then collected on a reel (Fig. 3A). NT  
62 dimerization stabilizes the fiber while CT amyloid-like fibril formation triggers solidification of  
63 the repetitive region (Fig. 2). [35, 36] This method of silk spinning has been shown to preserve  
64 beta-sheet formation and crosslinking tendencies of spidroins: 2Rep-sfGFP mixed NT2RepCT  
65 before spinning will attach to the main silk, tagging sfGFP while reinforcing the fiber.[36] This  
66 suggests that the nRep-xx fusion protein could potentially be used to tag peptides to recombinant  
67 spider silk.[36] HNP-1 is an impactful candidate.

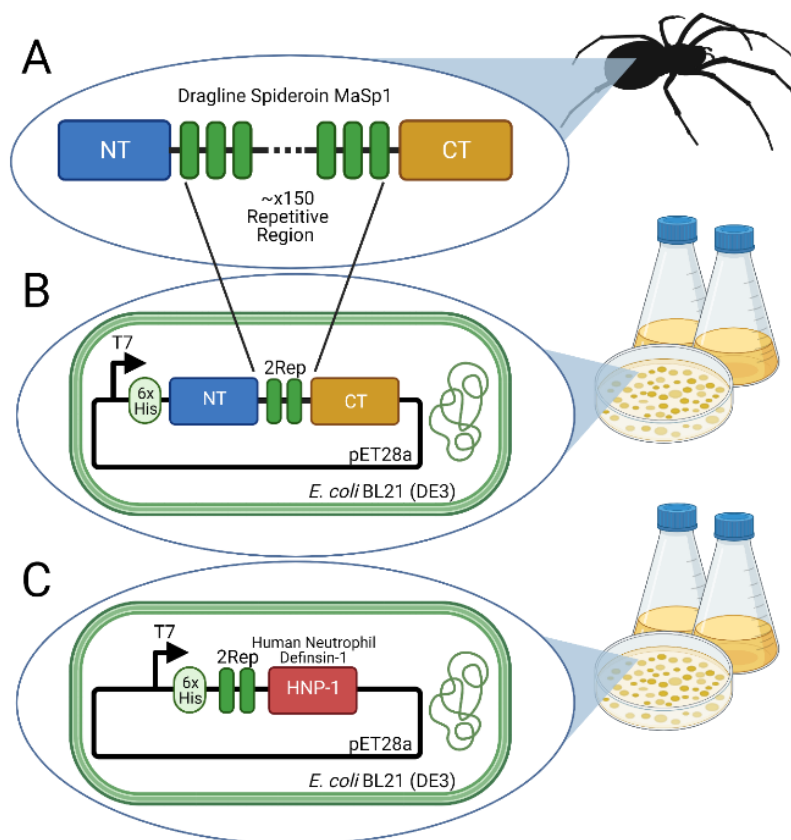


**Figure 1** Recombinant spidroin design. **A)** Spidroins have a large repetitive region, most notably with the Poly-A motif. **B)** Minispidroin NT2RepCT reduces the repetitive region and adds a 6xHis tag for purification. The chimeric NT and CT increase solubility. **C)** 2Rep-HNP1 fusion peptide in same construct

68 6mer-HNP1 (mer is another repeat) maintains broad range antimicrobial activity after a  
69 coagulating bath. It was designed as a post-spinning coating for Perma-Hand sutures, and cannot  
70 take advantage of the unique strength and extensibility spider silk offers. Furthermore, the high  
71 molecular weight of this toxic protein decreases yield. [10, 11]

72 This study investigates whether the novel fusion protein 2Rep-HNP1 (Fig. 1C) can be produced  
73 and spun with the chimeric minispidroin NT2RepCT to create a silk product that paves the road  
74 for an antimicrobial spider silk suture that reduces surgical site infections. If 2Rep-HNP1 with a  
75 growth inhibiting effect on *S. aureus* and *E. coli* is mixed with NT2RepCT and biomimetically  
76 spun into silk, the 2Rep domains will form beta-sheet linkages and create a stable antimicrobial  
77 recombinant spider silk (Fig. 2). Furthermore, efficiency of spidroin production, adjustable silk  
78 diameter, and spidroin “sheet” formation were investigated during experimentation to create a  
79 cohesive demonstration of the practicality and far-reaching potential of antimicrobial  
80 recombinant spider silk.

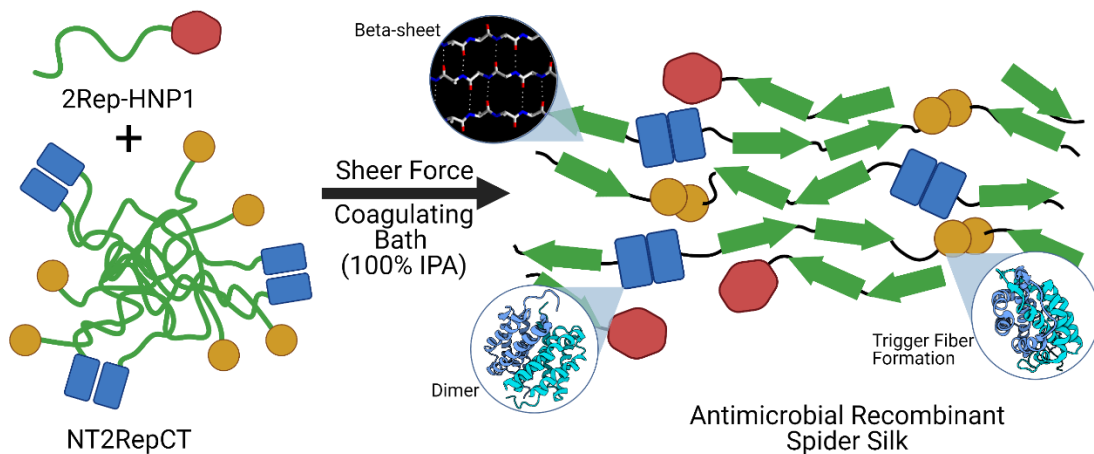


**Figure 2** Mechanism of 2Rep-HNP1 attachment and silk formation. In native state, NT2RepCT micelles can maintain solubility at high concentrations because of the chimeric soluble NT and CT. After passing through a 100% IPA bath with sheer force, NT dimerization helps connect separate NT2RepCT together, and CT amyloid-like fibril formation triggers silk formation, turning the repetitive region into antiparallel bonding beta-sheets. In a mixture of containing 2Rep-HNP1, beta-sheet hydrogen bonding between the 2Rep domains of 2Rep-HNP1 and NT2RepCT can connect the two together and create antimicrobial recombinant spider silk to be used in sutures.

### 81 3. Materials & Methods

#### 82 3.1. Design and synthesis of chimeric spidroins

83 The chimeric minispidroin NT2RepCT (BBa\_K3264000) is made of the N-terminal of the *E.*  
84 *australis* MaSp1 (AM259067), two repeats of the *E. australis* MaSp1 repetitive region

85 (AJ973155), and the C-terminal of the *A. ventricosus* MiSp1 (JX513956).[35] The fusion protein  
86 2Rep-HNP1 is made of two repeats of the *E. australis* MaSp1 repetitive region (AJ973155), and  
87 the Human Neutrophil Defensin-1 active peptide (P59665.1).[10] All segments are joined by  
88 GNS linkers, and a 6xHis (MGHHHHHH) tag was placed before the N terminal.[36] *E. coli*  
89 protein expression codon optimization was performed with GenSmart. Genes were synthesized  
90 and cloned into pET28a(+) vector by Genscript, and resuspended to 0.2 $\mu$ g/ $\mu$ L with ddH<sub>2</sub>O.

### 91 *3.2. Bacterial transformation and expression*

92 50 $\mu$ L aliquots of *E. coli* BL21(DE3) (Thermo Fisher) were mixed with 3 $\mu$ L of each plasmid with  
93 ddH<sub>2</sub>O as a control. Samples were incubated on ice for 30 min, 42C for 30 sec, and ice for 2  
94 min. 250 $\mu$ L of S.O.C. media was added to each sample and shaker incubated (New Brunswick,  
95 Eppendorf) at 37C 225rpm 1 hr. 50 $\mu$ L and 200 $\mu$ L aliquots were spread on LB-kanamycin  
96 (50 $\mu$ L/mL) agar plates and incubated overnight at 37C.

97 Inoculated starter cultures of 6mL LB-kanamycin that were shaker incubated at 37C 250rpm  
98 overnight were used to make 25% glycerol stocks and inoculate in a 1:50 ratio TB-kanamycin in  
99 baffled 1L flasks (Thermo Fisher). Cultures were shaker incubated at 37C 250rpm until OD<sub>600</sub>  
100 (Nanodrop, Thermo Fisher) was 0.6-0.8. NT2RepCT cultures were induced to 0.5mM IPTG, at  
101 25C 250rpm overnight. 2Rep-HNP1 cultures were induced to 1mM IPTG, at 37C 250rpm 4hrs.

102 Bacteria pellets were harvested by ultracentrifugation (Sorvall, Thermo Fisher) at 4C 7000xG  
103 15min, and twice washed with ice-cold PBS. NT2RepCT pellet was frozen -20C overnight, and  
104 2Rep-HNP1 pellet was resuspended in 1:10 culture volume of denaturing lysis buffer (100mM  
105 NaH<sub>2</sub>PO<sub>4</sub>, 10mM Tris HCl pH8, 8M urea, 1mM PMSF, 10mM imidazole, adjusted pH8.0) 4C  
106 overnight.[11] NT2RepCT was resuspended in 1:10 culture volume of native lysis buffer (20mM  
107 Tris HCl pH8, 500mM NaCl, 1mM PMSF, 10mM imidazole, 100ug/mL lysozyme) and  
108 incubated 4C for 30min. Both were sonicated at 40% power 6 x 30sec and ultracentrifuged at 4C  
109 13000xG 30min to recover lysate supernatant. Additional sonication and ultracentrifugation were  
110 performed if lysate was turbid.

### 111 *3.3. Ni-NTA affinity chromatography purification*

112 Native buffers in PBS with varying imidazole were prepared for NT2RepCT: equilibration  
113 (10mM), wash (20mM), elution 1 (100mM), elution 2 (250mM). Denaturing buffers in 100mM

114 NaH<sub>2</sub>PO<sub>4</sub>, 10mM Tris HCl pH8, 8M urea with varying imidazole and adjusted pH were  
115 prepared for 2Rep-HNP1: equilibration (10mM, pH8), wash (20mM, pH6.3), elution 1 (100mM,  
116 pH5.8), elution 2 (250mM, pH4.5).

117 Ni-NTA column resin (HisPur, Thermo Fisher) equilibrated with two resin-beds of equilibration  
118 buffer was added 1:20 lysate and end-over-end shaker (Thermo Fisher) incubated at 4C  
119 overnight. The mixture was added to chromatography column (Pierce, Thermo Fisher) and  
120 passed flow-through twice. Columns were washed with 20 resin-beds of equilibration buffer and  
121 10 resin-beds of wash buffer. Samples were eluted in 1 resin-bed fractions with 3 resin-beds of  
122 elution 1 buffer and 7 resin-beds of elution 2 buffer. SDS-PAGE of column fractions confirmed  
123 the protein of interest, using Tris-Gly 8-16% gels (Novex, Thermo Fisher) at 225V for 36  
124 minutes stained with Blazin Blue (Goldbio) and imaged with FluorChem R (ProteinSimple).

125 The 6 most concentrated fractions were concentrated and desalted with 6mL 3MWCO protein  
126 concentrator columns (Pierce, Thermo Fisher) at 4C 4000xg 4 hrs and stored at 4C. BCA  
127 working reagent (Pierce, Thermo Fisher) with a 1:20 BSA 2000, 1000, 500, 250, 125, 25, 0  
128 ug/mL standard curve and 1/500 and 1/1000 dilutions of concentrated protein in replicate was  
129 incubated at 37C for 30 minutes and measured at 562nm with Nanodrop One to find protein  
130 concentration and yield in mg/L culture.

### 131 *3.4. Biomimetic silk spinning*

132 NT2RepCT was diluted to 150mg/mL and 2Rep-HNP1 to 100mg/mL with 20mM Tris HCl pH8.  
133 Mixtures of 10%, 5%, 4% 2Rep-HNP1 with NT2RepCT and pure NT2RepCT were tested at 10-  
134 30μL/min with a 1mL (BD) syringe pump (Braintree Scientific) and 26G needle (BD)

135 The vertical pump ejected protein into a 100% isopropanol coagulating bath, and tweezers  
136 carefully collected continuous fibers and acted as a collection frame. Dried fibers were washed  
137 twice in ddH<sub>2</sub>O and stored at room temperature in petri dishes sealed with tape. Diameter  
138 measured after drying.

### 139 *3.5. Silk diameter characterization*

140 Prepared silk samples either in petri dish or on cardboard frame were viewed with the ZOE  
141 Fluorescent Cell Imager (Bio-Rad) in the brightfield and green channels. Random selections

142 were used to calculate the mean diameters of the silk with ImageJ. Performed with 12 duplicates  
143 per silk.

### 144 *3.6. Variable needle and rate spinning*

145 30 $\mu$ L samples of NT2RepCT were spun at 15 $\mu$ L/min with 24G, 26G, and 28G needles. Diameter  
146 measured after drying. 30 $\mu$ L sample of NT2RepCT was spun with rate increasing to 150 $\mu$ L/min  
147 with 26G needle. After drying, silk sheet was carefully torn apart to reveal internal structure.

### 148 *3.7. Silk degradation characterization*

149 Silk samples are too light to quantify with a milligram balance. Quantitative criteria for  
150 degradation were established: Intactness, diameter, overall size, comparison to control once dry.  
151 Control was dry room-temperature silk. All samples were washed twice with ddH<sub>2</sub>O and dried  
152 before testing.

153 Physiological conditions were mimicked with PBS pH7.4. Sterilization was mimicked with 70%  
154 ethanol. Samples were photographed, and incubated in 1mL solution at 37C for 3 days monitored  
155 daily. Dry-cycle steam autoclave 121C 20min was also used to mimic sterilization.

### 156 *3.8. Log reduction of S. aureus and E. coli CFU*

157 Antimicrobial ability of 2Rep-HNP1 was assessed with E. coli BL21(DE3) and S. aureus  
158 Rosenbach 6538 ATCC. [Note: 6538 is NOT a MRSA strain.] 6mL LB cultures were shaker  
159 incubated 37C 150rpm overnight, pelleted at 4C 10000xg 4 min, and washed twice with ice-cold  
160 PBS. Bacteria was resuspended in ice-cold PBS to a final OD<sub>600</sub>=0.3 measured with Nanodrop  
161 One. The OD<sub>600</sub>=0.3 suspensions were diluted to OD<sub>600</sub>=0.1 with PBS and 1:1 added to 50 $\mu$ L  
162 samples of 2Rep-HNP1 (50, 25mg/mL), and shaker incubated at 37C 150rpm for 24 hrs. 50 $\mu$ L  
163 serial dilutions (1/10, 1/100, 1/10000, 1/100000) into PBS were plated on LB agar and incubated  
164 at 37C for 24 hours. ddH<sub>2</sub>O and NT2RepCT were controls. Performed in duplicate. Log  
165 reduction of CFU was calculated using OpenCFU to count colonies.[40]

### 166 *3.9. Radial diffusion assay*

167 50uL of E. coli and S. aureus OD<sub>600</sub>=0.3 suspension was plated in LB Agar with a spreader.  
168 40uL of 2Rep-HNP1 (1mg/mL) was put on plates and incubated at 37C for 24 hrs. NT2RepCT  
169 was used as control. Performed in duplicate.

170 3.10. Analysis and figures

171 All data are given as mean  $\pm$  standard deviation unless noted otherwise. For analysis, one-way  
 172 ANOVA test and Tukey's multiple comparison test were performed, with  $p < 0.05$ . Graphs were  
 173 and plotted using GraphPad Prism 9.0. Schematics were made with BioRender.

174 4. Data & Results

175 4.1. Protein production with altered protocol

176 The final expression protocol used Terrific Broth expression media with 0.4% glycerol and 1:5  
 177 filled baffled 1L flasks. The final NT2RepCT native lysis buffer contained NaCl, a nonspecific  
 178 Ni-NTA binding reducer, PMSF, a protease inhibitor, and lysozyme, a supplement to sonication.  
 179 These additions were not harmful after desalting through 3k MWCO protein concentrator (Fig.  
 180 3A). BCA assay (Fig. 3B) calculated a concentration of  $295 \pm 2.7 \text{ mg/mL}$  and final yield of

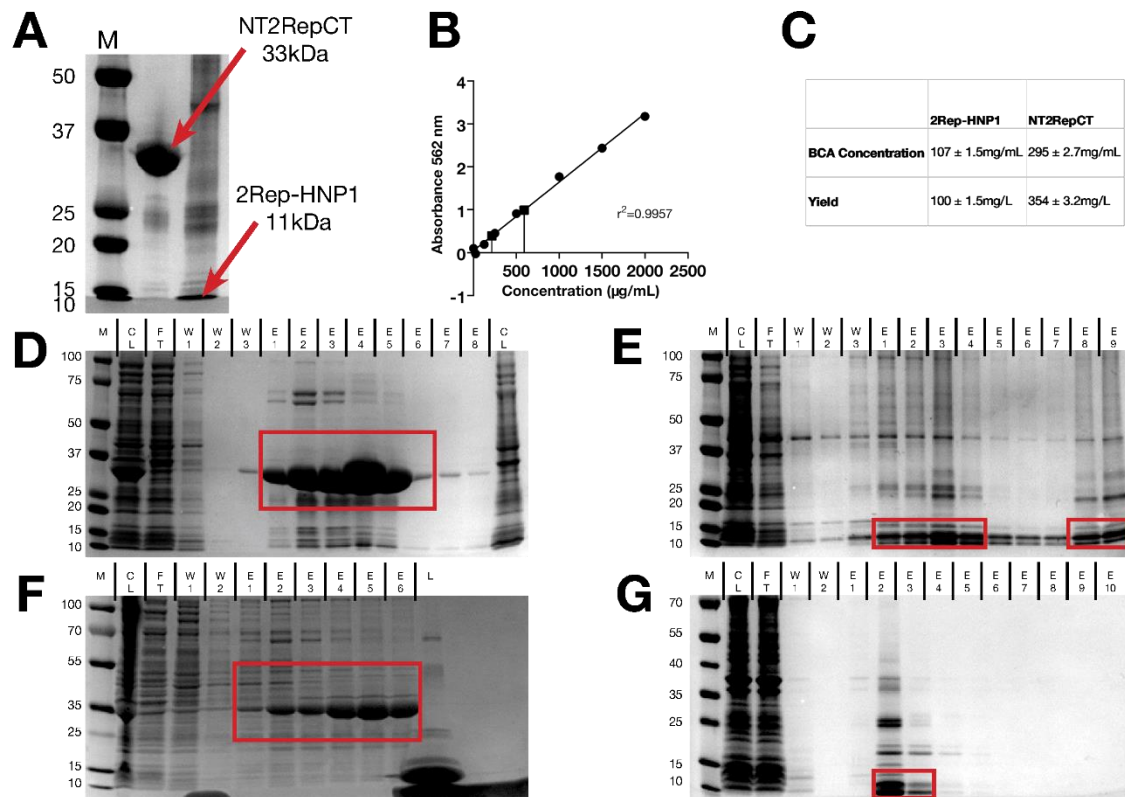


**Figure 3** Ni-NTA protein purification results. **A)** Confirmation of 3k MWCO dialyzed protein. **B)** BCA curve with interpolated 1/500 dilution concentrations. **C)** Protein concentration and yield. **D, E)** Modified protocol purification results for NT2RepCT and 2Rep-HNP1. **F, G)** Original protocol results with low yield. Boxed fractions were used in dialysis. **A** is 12% Tris-Gly, **DEFG** are 8-16% Tris-Gly. **M** for **ADE** is Bio-Rad Dual Color, **F** is Thermo PageRuler, **G** is Thermo PageRuler Plus. **F** lane "L" is 10kDa lysozyme.



181 354±3.2 mg/L of TB culture (Fig. 3C). This value is statistically significantly higher than the  
182 original publication 125mg/L and the hitherto highest reported yield of 336nm/L.[35, 36]

183 The 2Rep-HNP1 protocol was modified to denaturing lysis buffer and a shorter induction time of  
184 4hrs. BCA assay calculated a concentration of 107±1.5mg/mL and final yield of 100±1.5 mg/L  
185 of TB culture. After 7 runs final Ni-NTA purification with modified protocols (Fig. 3D, 3E) was  
186 much more efficient than original run (Fig. 3F, G).

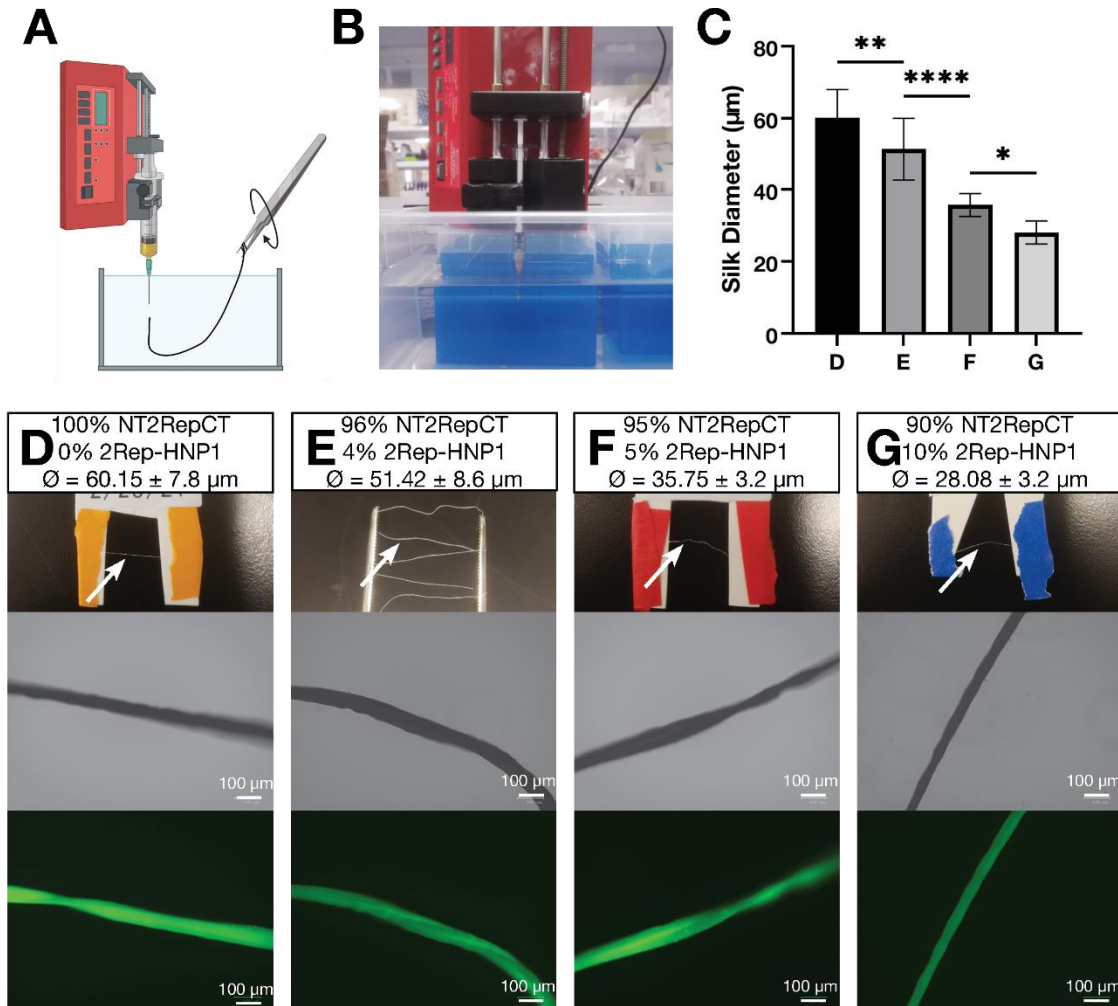
187 After desalting, NT2RepCT and 2Rep-HNP1 both did not precipitate at high concentrations, and  
188 did not degrade for at least 1 week stored at 4C and with constant use at room temperature.  
189 Dilution to working concentrations of 150mg/mL and 100mg/mL for NT2RepCT and 2Rep-  
190 HNP1 with 20mM Tris did not lead to precipitation either.

#### 191 *4.2. Silk spinning with variable conditions*

192 A simplified silk spinning device (Fig. 4A) was set up as described, with a bath of 100%  
193 isopropanol, syringe pump set to set to 15µg/min and with a 28G needle. Testing with only  
194 NT2RepCT revealed fiber formation was only possible when the needle was 5cm or from the  
195 container bottom (Fig. 4B), as solid silk must form during the short fall so it can be collected by  
196 tweezers (Fig. 5A).

197 Pure NT2RepCT (Fig. 4D, Fig.5B) had a mean diameter 60.15±7.8µm. Mixtures of 2Rep-HNP1  
198 and NT2RepCT were tried. 10% 2Rep-HNP1 (Fig. 4G) partially precipitated when mixed with  
199 NT2RepCT and was difficult to draw into the syringe. Silk was discontinuous, breaking after  
200 contact with the container bottom, or upon attempting to gather a longer continuous segment.  
201 The longest collectable length was 3.81 cm. The mean diameter was 28.08±3.2 µm. Mixtures of  
202 4% (Fig. 4E) and 5% (Fig. 4F) 2Rep-HNP1 had spinning properties similar to 100% NT2RepCT,  
203 with 4% less prone to breakage. The mean diameter of 4% silk was 51.42±8.6µm and the mean  
204 diameter of 5% silk was 35.75±3.2µm.

205 The statistically significant inverse relationship between 2Rep-HNP1 percentage and silk  
206 diameter (Fig. 4F) is accounted for by bonding of 2Rep-HNP1 to NT2RepCT denser  
207 crosslinking. [33, 36, 39] This demonstrates successful beta-sheet crosslinking. Explored more in  
208 discussion.



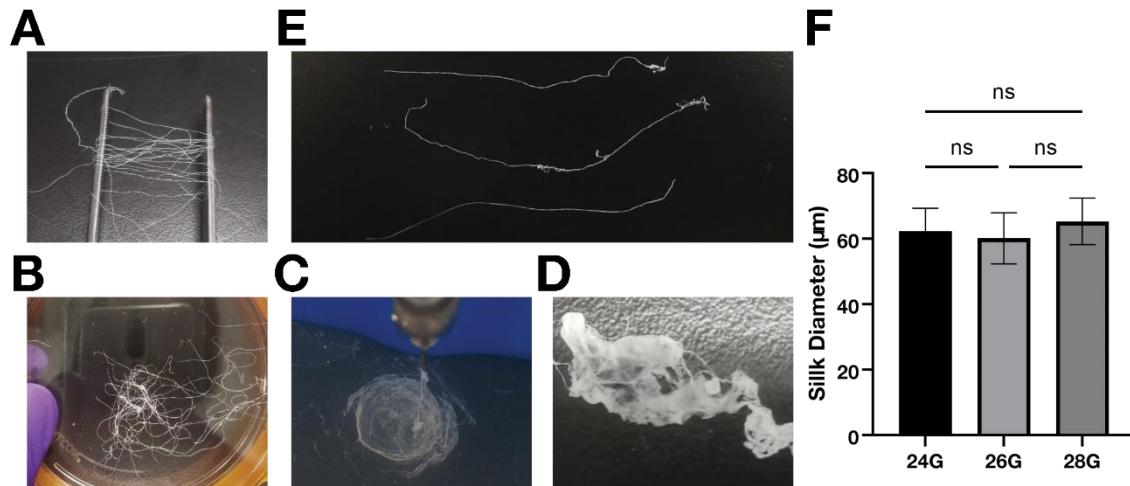
209

**Figure 4** Biomimetic spinning of spider silk. **A)** Silk spinning components: a syringe pump, a coagulating bath, and a collection rack. **B)** Equipment setup and minimum container depth. **C)** Statistically significant diameter differences of mixtures demonstrate successful beta-sheet bonding. **D, E, F, G)** Normal and brightfield/green channel

210

211 Pure NT2RepCT spun with a 26G (260 $\mu\text{m}$ ) needle had a mean diameter of  $60.15 \pm 7.8 \mu\text{m}$  when  
212 ejected at a rate of  $15 \mu\text{L}/\text{min}$ . Diameter did not significantly change with a 28G (184 $\mu\text{m}$ ) or 24G  
213 (311 $\mu\text{m}$ ) needle (Fig. 5C). This supports previous research findings between 32G and 34G  
214 needle use and demonstrates no correlation between silk diameter and needle diameter given a  
215 constant rate.[36]

216 Above 70 $\mu\text{L}/\text{min}$ , the syringe pump produced flat, circular sheets of solidified silk protein with a  
217 visibly uniform distribution (Fig. 5D). Pulling apart dried sheet revealed retention of fibrous  
218 properties (Fig. 5E), akin to tissues and other fiber-based materials.



219

**Figure 5** Supporting findings of silk spinning. **A)** Tweezer spinning frame. **B)** NT2RepCT silk in larger quantity. **C)** Circular sheet formed by rapid ejection. **D)** Dried sheet retains silk-like fibers. **E)** 4% silk degradation testing. Silks are control, second PBS 37C for 3 days, 70% EtOH 37C for 3 days. **F)** Needle diameter creates no significant difference in silk diameter.

220

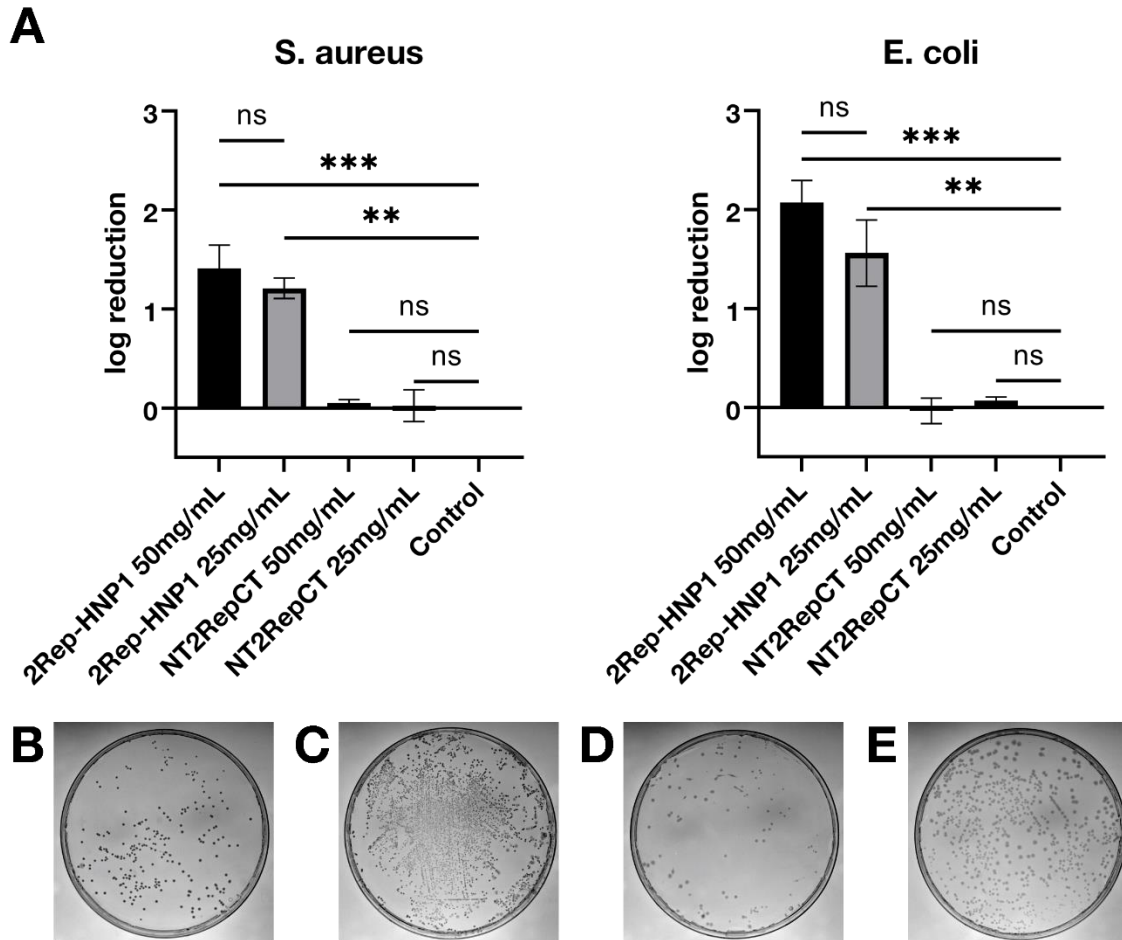
#### 221 4.3. Silk degradation conditions modeled in vitro

222 NT2RepCT and 4% 2Rep-HNP1 were incubated 37C for 3 days in PBS, 70% EtOH, or 20min in  
223 dry-cycle autoclave. After samples dried again, they were indistinguishable from the control  
224 according to criteria (Fig. 5E) and changes in silk diameter statistically insignificant.

#### 225 4.4. *S. aureus*, *E. coli* log reduction by 2Rep-HNP1

226 *S. aureus* Rosenbach 6538 ATCC and *E. coli* BL21 (DE3) log reduction ability of 2Rep-HNP1  
227 was tested at 50mg/mL and 25mg/mL, with no statistically significant difference in activity  
228 found. NT2RepCT had no effect on CFU log reduction, and has statistically significant  
229 difference in activity with 2Rep-HNP1 (Fig. 6A). Overall, for *S. aureus* 50mg/mL and 25mg/mL  
230 of 2Rep-HNP1 (Fig. 6B) had a 1.4-log and 1.2-log reduction, and 50mg/mL and 25mg/mL of  
231 NT2RepCT had a 0.05-log and 0.02-log reduction. For *E. coli* 50mg/mL and 25mg/mL of 2Rep-  
232 HNP1 (Fig. 6C) had a 2.1-log and 1.6-log reduction, and 50mg/mL and 25mg/mL of NT2RepCT  
233 had a -0.4-log and 0.07-log reduction. Control is 0 (Fig. 6 C, E). Log reduction demonstrates in  
234 liquid culture the broad-range antimicrobial activity of 2Rep-HNP1 against *S. aureus* and *E. coli*.

235 30µL of 1mg/mL 2Rep-HNP1 was dropped on spread plates of *S. aureus* and *E. coli* formed  
236 semi-visible zones of inhibition, further demonstrating the antimicrobial activity of 2Rep-HNP1  
237 in various conditions.



238

**Figure 6** Antimicrobial testing of 2Rep-HNP1 with log reduction assay. **A)** Log reduction of CFU with 2Rep-HNP1. Controls represent inoculated media diluted with ddH<sub>2</sub>O instead of protein. NT2RepCT are a second control so peptide presence is not confounding. 50mg/mL and 25mg/mL did not produce a statistically significant in log reduction, but all samples reduced CFU at least tenfold. Log reductions were calculated with log (CFU<sub>Control</sub>/CFU). **B)** CFU count in *S. aureus* treated with 2Rep-HNP1. **C)** Control for *S. aureus*. **D)** CFU count in *E. coli* treated with 2Rep-HNP1. **E)** Control for *E. coli*.

239

## 240 5. Discussion

241 Surgical site infections (SSI) represent a rising global health problem. Many infections come  
242 from surgical sutures, so antibiotic coated sutures have been developed in response. However,  
243 these hasten the antibiotic crisis and create harder to treat more lethal variants such as MRSA.  
244 Therefore, alternatives to antibiotic coated sutures must be researched.[5, 9-11] 2Rep-HNP1  
245 beta-sheet crosslinked to NT2RepCT combines the antimicrobial peptide properties of Human  
246 Neutrophil Defensin1 with the strength and elasticity that spider silk offers.[10, 14, 33, 36]

247 To validate the main hypothesis and demonstrate the feasibility of this approach, three important  
248 criteria were met: antimicrobial activity, beta-sheet crosslinking, and stability.

249 Direct antimicrobial silk testing requires 3m of unwoven silk per replicate, which is only  
250 possible in industrial or highly specialized settings.[35] Log reduction of liquid culture is known  
251 to be a good approximate for antimicrobial activity after silk spinning, which makes it more  
252 suitable for small-scale preliminary investigation.[10, 11] Results demonstrate the antimicrobial  
253 activity of 2Rep-HNP1 against *E. coli* or *S. aureus* is not affected by the addition of 2Rep (Fig.  
254 1C, Fig. 6), with reduction of at least 90% in both. This is consistent with antimicrobial 6mer-  
255 HNP1, and the fluorescent 2Rep-sfGFP, and supports that Rep does not interfere with protein  
256 functions in pre- and post- spinning.[11, 36] The broad-range action of 2Rep-HNP1 against both  
257 Gram-negative and Gram-positive bacteria further demonstrates viability in sutures.

258 The inverse relationship between 2Rep-HNP1 percentage and silk diameter (Fig. 4C) confirms  
259 2Rep beta-sheet crosslinking behavior (Fig. 2). Adding 2Rep-HNP1 to NT2RepCT causes  
260 crosslinking and creates a denser silk that may also be stronger, but overly high  
261 concentrations such as 10%, leads to precipitation and a discontinuous silk.[39] 4% silk is a good  
262 balance, being the most akin to pure NT2RepCT in terms of spinning properties and continuity,  
263 but is diameter difference shows 2Rep-HNP1 crosslinking still occurs. This shows modified  
264 2Rep proteins can bind to NT2RepCT and be spun into silk using a simple syringe pump.

265 Sutures experience a wide range of clinical conditions, and must not degrade at any point.  
266 NT2RepCT, 2Rep-HNP1, and all spidroin proteins depends on beta-sheet crosslinking and  
267 crystallinity, and a critical failure could endanger patients.[40] Both NT2RepCT and 4% silk was  
268 shown (Fig. 5E) to not degrade at physiological temperature 37C while suspended in  
269 physiological pH buffer, in 70% ethanol, or when autoclaved. These conditions model real-world  
270 use, and demonstrates spider silk has the stability required of suture products.

271 These criteria validate the hypothesis: The novel 2Rep-HNP1, with growth inhibiting effect on *S.*  
272 *aureus* and *E. coli*, can attach via 2Rep beta-sheet linkage to NT2RepCT and be spun into silk  
273 that is stable in surgery settings. This silk is a solution to SSI due to sutures. Other testing rounds  
274 out this model: efficient silk production for use at industrial scales, and alternate methods of silk  
275 formation and use.

276 Previous production methods for NT2RepCT have used LB and a simple lysis buffer, to a  
277 published yield of 125mg/L.[35] The well-designed chimeric terminals allow for extreme  
278 solubility, so higher yield methods are worth exploring. Production with TB and a more complex

279 lysis buffer increases yield to 354±mg/L (Fig. 3). This means 2.8km of silk can be spun with 1L  
280 of culture, a very efficient yield.[35] Ability of NT2RepCT and 2Rep-HNP1 to be stored at high  
281 concentration without special conditions lowers production costs. The high tolerance of needle  
282 diameter (Fig. 5F) for production of silk further lowers production cost. More efficient methods  
283 increase the likelihood of industrial production and product accessible, therefore real-world  
284 impact of antimicrobial recombinant spider silk.

285 Protein ejection rate alters the shape of the product into a “sheet”. This sheet still retains the  
286 fibrous nature of slower rate silk, but has a more random arrangement than woven silk and may  
287 be useful in situations were this is preferred, similar to paper structure. Sheets demonstrate how  
288 this protein combination can be adapted to any application where antimicrobial properties and  
289 the strength and flexibility of spider silk is needed, such as flexor tendon repair or liquid  
290 stiches.[41, 42]

## 291 **6. Conclusion**

292 2Rep-HNP1 and NT2RepCT form a stable antimicrobial spider silk material with potential use  
293 as sutures to solve surgical site infections. MRSA and other Gram-positive bacterial infections  
294 can be targeted by 2Rep-HNP1; this process does not disrupt HNP-1 function. Further testing  
295 provides a new protocol to increase yield of component proteins and supports the viability of  
296 industrial-scale production.

297 This provides evidence for a customizable, modular, functionalized spidroin 2Rep-xx. Not just  
298 antimicrobial peptides, any protein could potentially be added to NT2RepCT to create a strong  
299 silk with the properties of the added protein, or even of multiple mixed together. Further  
300 confirmation of the reliability of this method with other impactful proteins has the potential to  
301 usher in a new age of strong, elastic, spider silk-based biomaterials.

## 302 **7. Acknowledgements**

303 LabShares Newton and the Newton South High School Science Department provided lab space  
304 and materials. Snapgene provided software, Medsix provided the syringe pump, and BOA  
305 Biomedical provided *S. aureus*. S.L., H.S., and D.B. gave advice for science research. B.W.,  
306 Y.Y.C, J.L. provided purification and silk spinning advice. L.B. and M.L. assisted in literature  
307 review of AMP uses. S.L. reviewed manuscript.

## 308 **8. Attributions**

309 F.Y.C.L. conceived the original idea, performed all lab work, performed all analysis, and made  
310 manuscript and figures.

311 The author declares no competing interests.

312 Corresponding Author: Frank Y.C. Liu frankliuyc@gmail.com

## 313 **9. References**

- 314 1. Walter, J., et al., *Healthcare-associated pneumonia in acute care hospitals in European*  
315 *Union/European Economic Area countries: an analysis of data from a point prevalence survey,*  
316 *2011 to 2012.* Euro Surveill, 2018. **23**(32).
- 317 2. Anderson, D.J. and K.S. Kaye, *Staphylococcal surgical site infections.* Infect Dis Clin  
318 North Am, 2009. **23**(1): p. 53-72.
- 319 3. Stone, P.W., *Economic burden of healthcare-associated infections: an American*  
320 *perspective.* Expert Rev Pharmacoecon Outcomes Res, 2009. **9**(5): p. 417-22.
- 321 4. Fan, Y., et al., *The incidence and distribution of surgical site infection in mainland*  
322 *China: a meta-analysis of 84 prospective observational studies.* Sci Rep, 2014. **4**: p. 6783.
- 323 5. Tsai, D.M. and E.J. Caterson, *Current preventive measures for health-care associated*  
324 *surgical site infections: a review.* Patient Saf Surg, 2014. **8**(1): p. 42.
- 325 6. Ivanova, A., et al., *Layer-By-Layer Decorated Nanoparticles with Tunable Antibacterial*  
326 *and Antibiofilm Properties against Both Gram-Positive and Gram-Negative Bacteria.* ACS Appl  
327 Mater Interfaces, 2018. **10**(4): p. 3314-3323.
- 328 7. Yucel, T., M.L. Lovett, and D.L. Kaplan, *Silk-based biomaterials for sustained drug*  
329 *delivery.* J Control Release, 2014. **190**: p. 381-97.
- 330 8. Berkner, S., S. Konradi, and J. Schonfeld, *Antibiotic resistance and the environment--*  
331 *there and back again: Science & Society series on Science and Drugs.* EMBO Rep, 2014. **15**(7):  
332 p. 740-4.
- 333 9. Qian, Y., et al., *Surface Modified with a Host Defense Peptide-Mimicking beta-Peptide*  
334 *Polymer Kills Bacteria on Contact with High Efficacy.* ACS Appl Mater Interfaces, 2018.  
335 **10**(18): p. 15395-15400.
- 336 10. Franco, A.R., et al., *Silk-Based Antimicrobial Polymers as a New Platform to Design*  
337 *Drug-Free Materials to Impede Microbial Infections.* Macromol Biosci, 2018. **18**(12): p.  
338 e1800262.
- 339 11. Franco, A.R., et al., *Antimicrobial coating of spider silk to prevent bacterial attachment*  
340 *on silk surgical sutures.* Acta Biomater, 2019. **99**: p. 236-246.

- 341 12. Kamaruzzaman, N.F., et al., *Antimicrobial Polymers: The Potential Replacement of*  
342 *Existing Antibiotics?* Int J Mol Sci, 2019. **20**(11).
- 343 13. Hui, F. and C. Debiemme-Chouvy, *Antimicrobial N-halamine polymers and coatings: a*  
344 *review of their synthesis, characterization, and applications.* Biomacromolecules, 2013. **14**(3): p.  
345 585-601.
- 346 14. Gomes, S.C., et al., *Antimicrobial functionalized genetically engineered spider silk.*  
347 Biomaterials, 2011. **32**(18): p. 4255-66.
- 348 15. Deslouches, B. and Y.P. Di, *Antimicrobial Peptides: A Potential Therapeutic Option for*  
349 *Surgical Site Infections.* Clin Surg, 2017. **2**.
- 350 16. Casciaro, B., et al., *Promising Approaches to Optimize the Biological Properties of the*  
351 *Antimicrobial Peptide Esculentin-1a(1-21)NH<sub>2</sub>: Amino Acids Substitution and Conjugation to*  
352 *Nanoparticles.* Front Chem, 2017. **5**: p. 26.
- 353 17. Zasloff, M., *Antimicrobial peptides of multicellular organisms.* Nature, 2002. **415**(6870):  
354 p. 389-95.
- 355 18. Pachon-Ibanez, M.E., et al., *Perspectives for clinical use of engineered human host*  
356 *defense antimicrobial peptides.* FEMS Microbiol Rev, 2017. **41**(3): p. 323-342.
- 357 19. Varney, K.M., et al., *Turning defense into offense: defensin mimetics as novel antibiotics*  
358 *targeting lipid II.* PLoS Pathog, 2013. **9**(11): p. e1003732.
- 359 20. Tai, K.P., et al., *Microbicidal effects of alpha- and theta-defensins against antibiotic-*  
360 *resistant Staphylococcus aureus and Pseudomonas aeruginosa.* Innate Immun, 2015. **21**(1): p.  
361 17-29.
- 362 21. Sharma, S., I. Verma, and G.K. Khuller, *Therapeutic potential of human neutrophil*  
363 *peptide 1 against experimental tuberculosis.* Antimicrob Agents Chemother, 2001. **45**(2): p. 639-  
364 40.
- 365 22. Hardy, J.G., A. Leal-Egana, and T.R. Scheibel, *Engineered spider silk protein-based*  
366 *composites for drug delivery.* Macromol Biosci, 2013. **13**(10): p. 1431-7.
- 367 23. Aigner, T.B., E. DeSimone, and T. Scheibel, *Biomedical Applications of Recombinant*  
368 *Silk-Based Materials.* Adv Mater, 2018. **30**(19): p. e1704636.
- 369 24. Bern., N.H.M. *The World Spider Catalog, version 18.0.* Available from:  
370 <http://wsc.nmbe.ch/>.
- 371 25. Blackledge, T.A., et al., *Reconstructing web evolution and spider diversification in the*  
372 *molecular era.* Proc Natl Acad Sci U S A, 2009. **106**(13): p. 5229-34.
- 373 26. Agnarsson, I., M. Kuntner, and T.A. Blackledge, *Bioprospecting finds the toughest*  
374 *biological material: extraordinary silk from a giant riverine orb spider.* PLoS One, 2010. **5**(9):  
375 p. e11234.
- 376 27. Blackledge, T.A. and C.Y. Hayashi, *Silken toolkits: biomechanics of silk fibers spun by*  
377 *the orb web spider Argiope argentata (Fabricius 1775).* J Exp Biol, 2006. **209**(Pt 13): p. 2452-  
378 61.



- 379 28. Steven, E., et al., *Carbon nanotubes on a spider silk scaffold*. Nat Commun, 2013. **4**: p.  
380 2435.
- 381 29. Wright, S. and S.L. Goodacre, *Evidence for antimicrobial activity associated with*  
382 *common house spider silk*. BMC Res Notes, 2012. **5**: p. 326.
- 383 30. Askarieh, G., et al., *Self-assembly of spider silk proteins is controlled by a pH-sensitive*  
384 *relay*. Nature, 2010. **465**(7295): p. 236-8.
- 385 31. Hagn, F., et al., *A conserved spider silk domain acts as a molecular switch that controls*  
386 *fibre assembly*. Nature, 2010. **465**(7295): p. 239-42.
- 387 32. Rising, A., et al., *N-terminal nonrepetitive domain common to dragline, flagelliform, and*  
388 *cylindriform spider silk proteins*. Biomacromolecules, 2006. **7**(11): p. 3120-4.
- 389 33. Rising, A. and J. Johansson, *Toward spinning artificial spider silk*. Nat Chem Biol, 2015.  
390 **11**(5): p. 309-15.
- 391 34. Zhu, H., et al., *Tensile properties of synthetic pyriform spider silk fibers depend on the*  
392 *number of repetitive units as well as the presence of N- and C-terminal domains*. Int J Biol  
393 Macromol, 2020. **154**: p. 765-772.
- 394 35. Andersson, M., et al., *Biomimetic spinning of artificial spider silk from a chimeric*  
395 *minispidroin*. Nat Chem Biol, 2017. **13**(3): p. 262-264.
- 396 36. GreatBay\_SZ, *SPIDERMAN: SPIDroin EngineeRing with chromoprotein And Natural*  
397 *dye*. iGEM 2019, 2019.
- 398 37. Malay, A.D., K. Arakawa, and K. Numata, *Analysis of repetitive amino acid motifs*  
399 *reveals the essential features of spider dragline silk proteins*. PLoS One, 2017. **12**(8): p.  
400 e0183397.
- 401 38. Gosline, J.M., et al., *The mechanical design of spider silks: from fibroin sequence to*  
402 *mechanical function*. J Exp Biol, 1999. **202**(Pt 23): p. 3295-303.
- 403 39. Finnigan, W., et al., *The effect of terminal globular domains on the response of*  
404 *recombinant mini-spidroins to fiber spinning triggers*. Sci Rep, 2020. **10**(1): p. 10671.
- 405 40. Vepari, C. and D.L. Kaplan, *Silk as a Biomaterial*. Prog Polym Sci, 2007. **32**(8-9): p.  
406 991-1007.
- 407 41. Hennecke, K., et al., *Bundles of spider silk, braided into sutures, resist basic cyclic tests:*  
408 *potential use for flexor tendon repair*. PLoS One, 2013. **8**(4): p. e61100.
- 409 42. Annabi, N., et al., *Engineering a highly elastic human protein-based sealant for surgical*  
410 *applications*. Sci Transl Med, 2017. **9**(410).